Adaptable Energy Management System for Smart Buildings

Ilaria Salerno[a], Miguel F. Anjos[a,*], Kenneth McKinnon[a], Juan A. Gómez-Herrera[b]

[a] *School of Mathematics, University of Edinburgh, Peter Guthrie Tait Road, The King's Buildings, Edinburgh EH9 3FD, United Kingdom*
[b] *ExPretio Technologies, 200 Avenue Laurier Ouest, Montreal, QC H2T 2N8, Canada*

Abstract

This paper presents a novel adaptable energy management system for smart buildings. In this framework we model the energy consumption of a living unit, and its energy exchange with the surroundings. We explicitly consider the impact of the outside environment and design features such as building orientation, automatic shading, and double façade. We formulate this problem as a nonlinear optimization model in which the living unit minimizes a performance function subject to the energy flows from and toward the unit as well as the building-specific features. It is solved using off-the-shelf solvers. We present computational experiments to validate the proposed approach, considering different objective functions and several building configurations. The experiments show that our approach enhances the unit's performance and also provides demand flexibility for the grid.

Keywords: Demand Response, Nonlinear Programming, Building Design, Thermal Energy, Storage

1. Introduction

Electric energy systems must meet the demand for electricity while ensuring the security of the power system. This is particularly challenging during periods of high demand when the system is operating near its limits of both generation and transmission. When large-scale renewable generation options such as wind farms are connected to the grid, their fluctuating nature requires the system operator to keep more expensive generating units in reserve. These reserve units often use fossil fuels, leading to increased greenhouse gas (GHG) emissions and reduced benefit from the integration of renewable energy.

The alternative to using reserve generators is to increase the flexibility on the demand side of the electricity equation. This work is motivated by the potential for smart buildings of the (near) future to provide such flexibility. From the perspective of the

*Corresponding author
Email addresses: I.Salerno@sms.ac.ed.uk (Ilaria Salerno), anjos@stanfordalumni.org (Miguel F. Anjos), K.McKinnon@ed.ac.uk (Kenneth McKinnon), juan.gomez@polymtl.ca (Juan A. Gómez-Herrera)

grid operator, a building can be viewed as a means to store thermal energy via its use of electricity to operate various heating and cooling devices. This includes not only heating and air conditioning systems but also appliances such as refrigerators, freezers, and hot-water heaters. All this thermal storage capacity can be used to provide demand flexibility to the grid to the extent that the operation of these devices can be shifted in time, specifically into periods with lower demand.

Load shifting by users is generally referred to as demand–response (DR) or demand-side management (DSM). This is a well-known paradigm that has been used for many years to take advantage of the flexibility of large industrial consumers. More recently, the effectiveness of DR provision by hot-water heaters has been demonstrated by studies such as [1], and a mathematical optimization-based framework was proposed in [2, 3]. The advent of time-of-use (TOU) pricing for commercial and residential customers has partially tapped their DR potential.

Smart buildings offer the prospect of maximum utilization of the thermal storage potential of the built environment. Buildings have a significant impact on the overall energy consumption of a city [4], but individual buildings are unlikely to participate directly in DR because of their relatively small DR capacity. The pooling and coordination of their capacities is done via DR aggregators, or more generally, virtual power plants. These are commercial entities that perform near-real-time load shifting and more generally provide new ancillary services (these are the functions required to maintain grid stability). For example, customers in California can already participate in such DR aggregation [5].

Our contribution is a novel mathematical optimization framework (OF) that can model the full energy picture for a living unit from a range of residential buildings, including traditional houses, more energy-efficient units such as passive buildings, and buildings with a battery and their own energy generation (e.g., PV panels). Beyond modeling the energy consumption, the proposed OF accounts for the energy flows between the living unit and its surroundings. This means that it can consider the impact of the outside environment and of the design features such as automatic shading or a double façade. The objectives may be the total energy cost, the total energy consumption, the total GHG emissions, or some combination of these. From a broader perspective, the OF can in principle be used to predict each unit's energy demand, and hence the demand of a building. Being able to forecast the thermal behavior of a unit according to changing environmental conditions (weather, solar energy, activity inside the building) makes it possible to decrease the energy cost of the HVAC (heating, ventilation, and air conditioning systems) by up to 28% [6].

We demonstrate the capabilities and potential of the proposed OF using several case studies of user objectives and contexts. These highlight its adaptability to building design, its ability to account for the unit's geographical orientation, its potential for flexibility, and its adaptability to heating system operations.

This paper is structured as follows. Section 2 summarizes the relevant literature and background. Section 3 gives our notation, and Section 4 describes the proposed OF. Section 5 illustrates its capabilities and potential through four case studies. These consider the user's objectives; the OF's adaptability to building design; its ability to account for external factors such as geographical orientation and its potential for flexibility via DR; and its adaptability to heating-system operations. Section 6 provides concluding remarks.

2. Literature review

Three main fields merge in this paper: operational research (OR) applied to energy in buildings, energy storage, and building design.

2.1. Operational research applied to energy in buildings

The continuous development of smart grids has expanded the opportunities for OR to support decision-making across the grid, particularly on the consumption side. Data-gathering devices and the Internet of Things allow end-users to manage their own energy consumption, providing them with the ability to make smart independent decisions. There are various OR-based approaches that minimize the energy cost for residential users while providing DR services. The tutorial [7] presents a comprehensive review of OR for DR in buildings. The approaches include integer programming, stochastic optimization, simulation, and forecasting.

Local decision-making represents a coordination challenge since the aggregated behavior of multiple end-users can have a negative impact on the operation and economic performance of the grid. Several authors [8, 9, 10] focus on the optimal coordination of many users. They often define demand profile and user preferences for each household; aspects such as building design and orientation are typically neglected since the households are assumed to be identical. Additionally, decentralized generation such as solar and wind combined with storage resources and local decision-making have encouraged the development of *prosumers*: customers with enough generation capacity to potentially disconnect from the grid and satisfy their demand autonomously. The economic and market frameworks must be adjusted to efficiently integrate prosumers [11]. This has motivated several OR approaches that focus on the role of smart buildings in a market with prosumers. Zafar et al. [12] discuss information technologies and optimization techniques to support energy sharing among prosumers. Simulated annealing has been used [13] to determine optimal energy management strategies for neighboring prosumer buildings, while Iria and Soares [14] investigate the integration of an aggregator of prosumers in the day-ahead market. Approaches based on model predictive control (MPC) have shown that this technique can improve energy management in buildings. MPC can reduce the energy cost and power peaks of a small commercial building over a year, even if acting only on the heating system [15]. An approach integrating control and integer programming was proposed in [16].

2.2. Thermal energy storage

Thermal energy storage (TES) provides an interesting opportunity for the optimization of energy use. It has the potential to reduce the use of nonrenewable energy resources [17, 18], improve grid operations, reduce the heating/cooling consumption of buildings, and increase thermal comfort. TES can be an active or passive element of the heating system. It is passive if the charging and discharging cycles rely on thermal inertia or natural convection.

Alva et al. [17] classify TES in buildings. Passive TES benefits from the sensible or latent thermal mass of certain materials. The use of phase change materials (PCM) to control indoor comfort is an example: their thermal mass smooths the fluctuation of the external temperature. Active TES works in combination with other components, such as HVAC systems, the structure of the building, or the surrounding environment. Examples

include the water storage tanks of the HVAC system and aquifer storage in the vicinity. Passive TES and HVAC storage are the most common technologies used in buildings. Common materials include water or sand, and PCM for low-temperature applications.

TES provides significant energy savings. Parameshwaran et al. [18] found that a combination of latent heat energy storage and active cool TES systems can reduce the space conditioning consumption of a building by 45–55%. They suggest that TES may lead to long-term cost savings, but it is necessary to standardize the performance for different climates and policies. TES is an efficient tool for internal comfort, with a minimal impact on the environment. It often enables buildings to earn the Leadership in Energy and Environmental Design (LEED) certification, because it lowers GHG emissions and improves energy efficiency [18].

There is a growing interest in the use of TES to provide flexibility to the grid. One of the challenges is to measure this flexibility. Stinner et al. [19] quantify the flexibility via a method based on time, power, and energy; they consider the average power cycle and the flexibility per year. They show that power and energy output mainly depend on the capacity of the heat generator; TES size does not have a significant impact. On the other hand, the duration of the flexibility depends more on the TES size than on the generator features.

In this paper we focus on small-scale TES, according to the classification in [20]. Small-scale TES systems have a short charging cycle and a low energy capacity. This technology is an efficient tool for buildings, especially if it is integrated into their structure [20]. There have been many studies of TES, but few address its integration into the building. We use the building itself as passive TES: the OF uses the thermal masses of the building's elements as passive storage. Furthermore, some of these thermal masses become active TES: the OF benefits from them by ventilating or by running a local heat pump (HP).

2.3. Building design

Passive Building Design. Passive building design is a set of principles that apply to all building types. Passive buildings are characterized by high energy efficiency because of their low energy consumption. Such a building may be referred to as a *Passivehaus*, *Zero-energy home*, *Maison autonome en énergie*, or *Green building*. Filippi and Fabrizio [21] suggest the following definitions: the Passivehaus focuses on the improvement of solar gains and is characterized by heating energy below 15 $\mathrm{kWh/m^2year}$; the Maison autonome en énergie is an off-grid building that is autonomous in terms of energy; the Green building respects a green standard such as LEED; and the Zero-energy home may or may not be connected to the grid and controls the total annual consumption (not only heating). The 2010 European Directive [22] promotes the development of near-zero-energy buildings that primarily use energy from nearby renewable sources.

Passive building design is attracting increasing interest. Moran et al. [23] found that focusing on minimizing the heating demand by reducing thermal losses throughout the envelope is the best way to improve energy efficiency. Only after that can renewable energy integration be efficiently planned. Several passive buildings have been built [24], and Italy is in the vanguard. The zero-energy house in Felettano di Tricesimo (UD) is a beautiful "Home Sapiens" designed in 2010 that controls its energy resources via its home automation system. The primary school by the architect Vonmetz in Lajon (Sud Tirolo) is the first passive school building in Italy; it won a CasaClima award in 2006.

Passive buildings allow their owners to both reduce costs and improve comfort (measured as the level of satisfaction). The construction cost must be taken into account. Colclough et al. [25] compared 20 dwellings, 11 passive and 9 standard, and concluded that passive buildings are generally cheaper to construct than standard buildings.

We apply the proposed OF to a passive building with a double skin façade (DSF) and dynamic shading in the air gap. We next review these two technologies.

Double skin façade. A DSF is one of the best ways to efficiently manage the energy needs of a building [26]. It impacts the heating, cooling, lighting, and ventilation loads, and it can boost energy savings. Darkwa et al. [27] discuss the advantages of a DSF: energy reduction, increased ventilation and thermal comfort, and glare control. A DSF positively affects acoustic insulation and aesthetic appeal, increasing the building's value. Moreover, the durability of DSF technology [28] lowers the building's long-term cost.

Adding a DSF to a building is cheaper and less intrusive than demolition and reconstruction. Pomponi et al. [29] studied the refurbishment of an office building in London. They compared 128 DSF configurations and 8 single-skin solutions, and in 98.4% of the scenarios, DSF outperformed single-skin in terms of energy savings. Furthermore, in 83% of the scenarios, DSF had lower carbon emissions. Haase and Wigenstad [30] studied the refurbishment of an office building in Norway. They compared a single-skin solution to two DSFs with different types of glass. The DSF options performed better in both energy savings (49% and 59%) and thermal comfort.

The DSF can be common to the entire surface or in several smaller parts. We model smaller independent spaces, one per dwelling, to illustrate the adaptability of the system. Moreover, we study the overall performance of the building.

Smart shading. We use smart shading to control the intake of solar energy. This takes the form of automatic blinds that open and close as desired. This increases the energy efficiency and improves visual and thermal comfort. Konstantoglou and Tsangrassoulis [31] show that the efficiency of such a dynamic façade depends on how well it is integrated with the lighting and heating/cooling systems. The automatic control should take into account the temperature inside the living zone (LZ) and the quantity of solar gains. They find overall energy savings of around 20% for the cooling consumption and 50% for lighting.

To the best of our knowledge, mathematical optimization has never been used to optimize the control of dynamic shading in order to improve energy operations. We demonstrate the adaptability of the proposed OF by considering the effect of dynamic shading on the internal temperature of the unit. The smart shading optimally adapts to the available solar energy and the thermal comfort inside the unit, while also maintaining visual comfort.

3. Notation for the optimization framework

We use uppercase characters for the variables and lowercase for the parameters.

Sets.

- $\mathcal{I}$ set of time frames, indexed by i

- $\mathcal{B}$ set of nodes, indexed by b
- $\mathcal{G}$ set of energy resources, indexed by g
- $\mathcal{S}$ set of thermal storage, indexed by s
- $\mathcal{L}$ set of lines, indexed by l
- $\mathcal{W}$ subset of lines, crossed by conserved flow, indexed by $l \in \mathcal{L}$
- $\mathcal{H}$ subset of lines, crossed by nonconserved flow, indexed by $l \in \mathcal{L}$

Parameters.

- F_l : node $b \in \mathcal{B}$ where line l starts
- T_l : node $b \in \mathcal{B}$ where line l ends
- B_g : node $b \in \mathcal{B}$ where energy resource g is connected
- B_s : node $b \in \mathcal{B}$ where storage s is connected
- r_l : thermal resistance of line l [m^2 K/kW]
- $q_{i,g}^{int}$: power generated by people, electronic devices, and lighting during time frame i [kW]
- $q_{i,g}^{sol,B}$: power generated by the direct component of solar rays during time frame i [kW]
- $q_{i,g}^{sol,D}$: power generated by the diffuse component of solar rays during time frame i [kW]
- ϵ_g : clearness index of smart shading, acting on resource g, during time frame i [-]
- y_s : heat capacity of storage $s \in \mathcal{S}$ [kJ/(K s)]
- y_l^{air} : heat capacity of air mass flowing in line l [kJ/(K s)]
- $\Delta_{i,g}^{min}$: minimum value of $\Delta_{i,g}$ related to resource g during time frame i [-]
- $\Delta_{i,g}^{max}$: maximum value of $\Delta_{i,g}$ related to resource g during time frame i [-]
- $t_{i,b}^{min}$: minimum value of temperature $T_{i,b}$ in node b during time frame i [-]
- $t_{i,b}^{max}$: maximum value of temperature $T_{i,b}$ in node b during time frame i [-]
- $p_{i,l}^{W}$: maximum power input of line l during time frame i [kW]

Variables.

- $T_{i,b}$: temperature of node b during time frame i [°C]
- $P^{L}_{i,l}$: power in line l, from node F_l to node T_l, during time frame i [kW]
- $P^{H,T}_{i,l}$: power reaching node T_l of line l during time frame i [kW]
- $P^{H,F}_{i,l}$: power leaving node F_l of line l during time frame i [kW]
- $P^{G}_{i,b}$: sum of power from generators connected to node b during time frame i [kW]
- $P^{S}_{i,s}$: power flowing to/from storage s during time frame i [kW]
- $P^{V}_{i,l}$: ventilation air flow in line l during time frame i [kW]
- $W_{i,l}$: electricity input to the heat pump represented by line l [kW]
- $Q^{sol}_{i,g}$: power generated by solar rays during time frame i [kW]
- $\Delta_{i,g}$: coefficient of smart shading related to power generated by resource g during time frame i [-]
- $L_{i,s}$: level of energy stored in storage s during time frame i [kWh]
- $X_{i,l}$: air exchange rate of the ventilation represented by line l during time frame i [-]
- E_l : efficiency of a heat pump l. This depends on its working temperatures T_{i,F_l} and T_{i,T_l} in each time period i [-]

4. Optimization Framework

The OF is a nonlinear optimization model, and its structure is inspired by two well-known modeling paradigms. First, we view the building as an energy network of buses linked by lines, but instead of electric energy, heat flows between the buses. Second, we represent components in the network using RC electrical circuit analogies to the building's thermal features. This approach makes the OF flexible and easily applicable in different contexts and with different objectives.

Figure 1 illustrates a simple instance of the energy flow network. The nodes (or buses) of the OF represent elements with thermal capacity. Furthermore, they are associated with temperature values. The nodes are connected by lines on which power flows (the blue arrows in Fig. 1). On each line, power may be lost or conserved. The lines connecting the nodes can be balanced or unbalanced and controlled or uncontrolled. The line is balanced if the flow leaving one end is equal to the flow arriving at the other end. Heat exchange between two nodes is an example of a balanced line. The line is controlled if the OF decides the timing and quantity of the flow; ventilation is an example. In this representation, temperature plays the role of voltage in a circuit: if the temperatures of the two nodes connected by a line are different, then power flows from one node to the other. This is a balanced and uncontrolled line (P^{L}_{l} in Fig. 1); an example is heat

exchange between two materials. Each line has a resistance, which is a parameter of the optimization model; these resistances are indicated by rectangles in Fig. 1 and denoted as r_l.

Ventilation is a balanced and controlled line. Power flowing from one node to the other (P_l^V) varies according to the variable $x_{i,l}$ and the parameter y_l^{air}, representing the air exchange rate and the air thermal capacity respectively.

The flow is unbalanced (P_l^H) when the power leaving the node at one end of a line is different from the power reaching the other end; an example is the behavior of an HP. The electricity input required by the HP is indicated by a yellow arrow in Fig. 1. Moreover, the HP line is associated with a function that represents its energy efficiency (E_l): this is the difference between the power leaving one end and that arriving at the other end of the line.

Each node can store energy. This is analogous to a capacitor in a circuit, and storage is represented by two parallel lines in Fig. 1. The heat capacity (or thermal mass) of a node is denoted y_s, and it is a property of the material.

A node can receive power from one or more external sources, referred to as generators. Sun radiation and heat from people and electrical devices are external resources. The sun radiation is controlled by the variable $\Delta_{i,g}$ and scaled by the parameter ϵ_g. These represent the status of the smart shading system and the clearness index of the external environment.

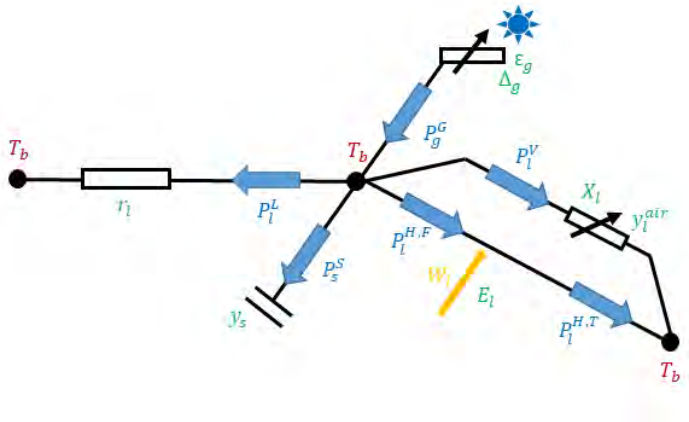

Figure 1: Visualization of OF operations.

Objective function.

$$\min \quad \sum_{l\in\mathcal{L}} \sum_{i\in\mathcal{I}} c_i W_{i,l} \tag{1}$$

The objective of the OF minimizes the product of $c_i W_{i,l}$, where $\sum_{l\in\mathcal{L}} \sum_{i\in\mathcal{I}} W_{i,l}$ is the overall electricity input of the heating/cooling system during the total running period. Depending on the values of c_i, the OF can minimize the total electricity cost, the total energy consumption, or the GHG emissions.

Constraints.
Balance, node b:

$$\sum_{l\in\mathcal{W}|b=T_l} P^L_{i,l} - \sum_{l\in\mathcal{W}|b=F_l} P^L_{i,l} + \sum_{l\in\mathcal{H}|b=T_l} P^{H,T}_{i,l} - \sum_{l\in\mathcal{H}|b=F_l} P^{H,F}_{i,l} +$$

$$+ \sum_{l\in\mathcal{W}|b=T_l} P^V_{i,l} - \sum_{l\in\mathcal{W}|b=F_l} P^V_{i,l} +$$

$$+P^G_{i,b} - \sum_{s\in\mathcal{S}|b=B_s} P^S_{i,s} = 0 \quad \forall i \in \mathcal{I}, \forall b \in \mathcal{B} \tag{2}$$

Branch flows:

$$P^L_{i,l} = \frac{1}{r_l}(T_{i,F_l} - T_{i,T_l}) \quad \forall i \in \mathcal{I}, \forall l \in \mathcal{W} \tag{3}$$

$$P^{H,T}_{i,l} = E_l(T_{i,F_l}, T_{i,T_l})W_{i,l} \quad \forall i \in \mathcal{I}, \forall l \in \mathcal{H} \tag{4}$$

$$P^{H,F}_{i,l} = P^{H,T}_{i,l} - W_{i,l} \quad \forall i \in \mathcal{I}, \forall l \in \mathcal{H} \tag{5}$$

$$P^V_{i,l} = X_{i,l}\ y^{air}_l\ (T_{i,F_l} - T_{i,T_l}) \quad \forall i \in \mathcal{I}, \forall l \in \mathcal{W} \tag{6}$$

Air change per hour in ventilation lines:

$$X^{min}_{i,l} \leq X_{i,l} \leq X^{max}_{i,l} \quad \forall i \in \mathcal{I}, \forall l \in \mathcal{W} \tag{7}$$

Constraint (2) ensures that the total power flowing into and out of each node is equal to zero. Power flows represent thermal fluxes, and we assume that the power flowing into a node has a positive sign.

There are five main types of flows. The first type is the power naturally flowing through a line, from a higher to lower temperature node: this balanced and uncontrolled flow is represented by the first two terms of (2) and by (3).

The second type of flow is similar, but it is unbalanced. It is represented by the third and fourth terms in (2) and by (4) and (5). These unbalanced lines simulate the heating/cooling system of the unit, by one or more HPs. Power flows from the colder to the warmer node. This process requires a certain amount of work, which is represented by the variable $W_{i,l}$. Equation (5) describes the energy conservation of the HP system: the amount of heat allocated to the hot node ($P^{H,T}_{i,l}$) must equal the amount of heat taken from the cold node ($P^{H,F}_{i,l}$) plus the work ($W_{i,l}$). The efficiency of this process depends on the temperature of the two nodes at the ends of the HP line. This dependence is described by (4). The output of the HP ($P^{H,T}_{i,l}$) is equal to its electricity input ($W_{i,l}$) times a function that represents the HP's energy efficiency (E_l). This efficiency (E_l) is a nonlinear function of the temperatures of the nodes to which it is connected (T_{i,F_l} and T_{i,T_l}).

The third category of flow is balanced and controlled ($P^V_{i,l}$ in Equations 2 and 6). It represents ventilation and simulates the air flowing from the warmer to the cooler node. The difference between this and the first type of flow is that ventilation is associated

with a variable ($X_{i,l}$) that represents the "air change per hour" (ACH). It ranges within bounds that guarantee comfort and hygiene inside the room (7). The ventilation flow depends on the amount of ventilated air ($X_{i,l}\ y_l^{air}$) and on the difference between the two nodes at the extremes of the line: ($T_{i,F_l} - T_{i,T_l}$). Moreover, y_l^{air} denotes the thermal mass of the air flowing in the ventilation line (6). The OF is nonlinear because of the ventilation constraint (6) and the HP constraint (4).

Heat energy from generators:

$$P_{i,b}^G = \sum_{g \in \mathcal{G} | b = B_g} (q_{i,g}^{int} + Q_{i,g}^{sol}) \quad \forall i \in \mathcal{I}, \forall b \in \mathcal{B} \tag{8}$$

Solar gains:

$$Q_{i,g}^{sol} = \Delta_{i,g} \epsilon_g (q_{i,g}^{sol,B} + q_{i,g}^{sol,D}) \quad \forall i \in \mathcal{I}, \forall g \in \mathcal{G} \tag{9}$$

Smart shading system configuration:

$$\Delta_{i,g}^{min} \leq \Delta_{i,g} \leq \Delta_{i,g}^{max} \quad \forall i \in \mathcal{I}, \forall g \in \mathcal{G} \tag{10}$$

Energy storage:

$$L_{i,s} = y_s T_{i,B_s} \quad \forall i \in \mathcal{I}, \forall s \in \mathcal{S} \tag{11}$$

Storage level of charge:

$$L_{i,s} = L_{(i-1),s} + P_{i,s}^S h \quad \forall i \in \mathcal{I}, \forall s \in \mathcal{S} \tag{12}$$

The fourth type of flow comes from a generator. It is denoted by $P_{i,g}^G$ in (2) and defined in (8). The power generation in the unit derives from sun rays ($Q_{i,g}^{sol}$), people, electronic devices, and the lighting system ($q_{i,g}^{int}$). During the heating periods, these elements are free and sustainable energy resources, because they warm up the unit. During the cooling periods we may want to reduce them because they represent an additional load. Accordingly, the OF can simulate a smart shading system. The variable $\Delta_{i,g}$ controls the solar power entering the unit, and (10) gives bounds on its value. This guarantees visual comfort inside the room. Clouds may reduce the solar penetration, and the parameter ϵ is the clearness index.

The fifth type of flow consists of power flowing into/out of a storage unit ($P_{i,s}^S$). Each node has an associated temperature and thermal mass. The thermal mass acts as thermal storage: it can be charged and discharged during different time frames (h in 12). This process is described by (11) and (12), where $L_{i,s}$ is the energy stored in the node. It depends on both the temperature ($T_{i,s}$) and heat capacity (y_s) of the node. Only changes in energy are relevant to the model, so the zero point can be chosen arbitrarily. We choose the zero point to correspond to a temperature of zero.

Temperature limit:

$$t_{i,b}^{min} \leq T_{i,b} \leq t_{i,b}^{max} \quad \forall i \in \mathcal{I}, \forall b \in \mathcal{B} \tag{13}$$

Ramping limit:

$$-l_b^D \leq T_{i,b} - T_{(i-1),b} \leq l_b^U \quad \forall i \in \mathcal{I}, \forall b \in \mathcal{B} \tag{14}$$

Power limit:

$$0 \leq W_{i,l} \leq p_{i,l}^{W} \quad \forall i \in \mathcal{I}, \forall l \in \mathcal{H} \tag{15}$$

Constraints (13), (14), and (15) control the operational limits of the unit. Equation (13) ensures that the node temperature stays within specified bounds. Equation (14) limits the rate at which the temperature varies. Accordingly, these two constraints may be applied to guarantee thermal limits. Constraint (15) ensures that the power flowing on the lines is within the operational capacity.

5. Applications of the OF

In this section we apply the OF to four study cases, with the aim to show its potential in real-world scenarios and its flexibility in dealing with different user's objectives, building designs, external factors and heating system configurations. Section 5.1 illustrates OF's adaptability to user's objectives, showing how it can be use as a simulator or as an optimizer to minimize either the energy consumption or the cost for a given tariff structure. Section 5.2 shows how the OF can be easily adapted to different building designs. We compare a building with a conventional external brick wall with one that has a double façade, consisting of the same traditional wall and an outer glass curtain wall with smart shading in between. Section 5.3 considers units with different orientations and shows how the OF adjusts optimally to these different environments. Finally Section 5.4 shows how the OF can be used to optimize different configurations of the heating system. This is illustrated by two cases, one with a single heat pump and one with two heat pumps in different locations.

5.1. User objectives

In this section we show how the OF can be used to model different environmental conditions and user objectives related to energy use and cost.

First, we apply the OF to what we call the "TRAD" unit: an apartment without an EMS. Here the OF acts as a load simulator: it outputs the heating/cooling energy consumption of the apartment, with a fixed room temperature profile. Second, we apply the OF to the "SM" (standard model) unit, which is TRAD with an EMS. We run the OF of the SM unit twice. In the first case, the EMS minimizes the cost of heating over a two-day period. In the second case, it minimizes the heating consumption while maintaining the temperature within defined limits.

TRAD and SM units. All the simulations are for the same apartment: a residential unit in Montreal (Canada) with one south-oriented external façade: see Fig. 2. Its heating/cooling demand is met by an HP. We model the HP with a dynamic efficiency (E_l) that varies according to its working temperature. We assume that the HP is centralized at the building level and operates between the external and internal temperatures.

The simulations run for two typical winter days, and within these days E_l is in the range 3.1 to 4.0. We calculate the electricity cost using the tariff structure shown in Fig. 5.

All the simulations consider ventilation between the exterior and interior, and this is optimized by the OF. The models account for heat transfer by conduction, convection,

and radiation. Convection and radiation are linearized and simplified, as suggested in [32].

Figure 2 shows the RC circuit corresponding to the TRAD and SM units. There are five nodes, each of which is associated with a temperature. We discuss them from right to left. Node 1 (t^{ext}) represents the external temperature; node 2 (T^{wall}) is the center of the external wall; node 3 (T^{int}) is the LZ; node 4 ($T^{intWalls}$) is the center of the internal walls and ceilings; and node 5 (T^{next}) represents the neighbors.

Balanced flow ($P^L_{i,l}$) takes place on the black lines connecting the nodes. They are characterized by fixed thermal resistances, defined for the structure of the unit (walls, windows, and air). Each black line represents half of the thickness of a wall/window/ceiling, and the flow ($P^L_{i,l}$)is balanced and uncontrolled. The purple line represents ventilation between nodes 1 and 3. The heat flow ($P^V_{i,l}$) is balanced and controlled by the OF using the variable $X_{i,l}$. The heat flowing between nodes also depends on the temperature difference between the nodes and the thermal capacity of the volume of air flowing y^{air}_l. The yellow line represents the HP connecting nodes 1 and 3. The flow is unbalanced ($P^{H,F}_{i,l}$ and $P^{H,T}_{i,l}$).

Each internal node has an associated storage due to its thermal mass (y_s). Because the heat flows to or from the unit do not affect the external temperature, this temperature is independent and assumed to be known. Accordingly, there is no need to model storage at this node. Furthermore, the generation power ($P^G_{i,g}$) is connected to node 3. It represents heat flows due to solar radiation, people, and electrical devices. Node 5 represents the neighbor's internal temperature. It may vary within the range of the LZ temperature T_{int} (13), which defines the thermal comfort.

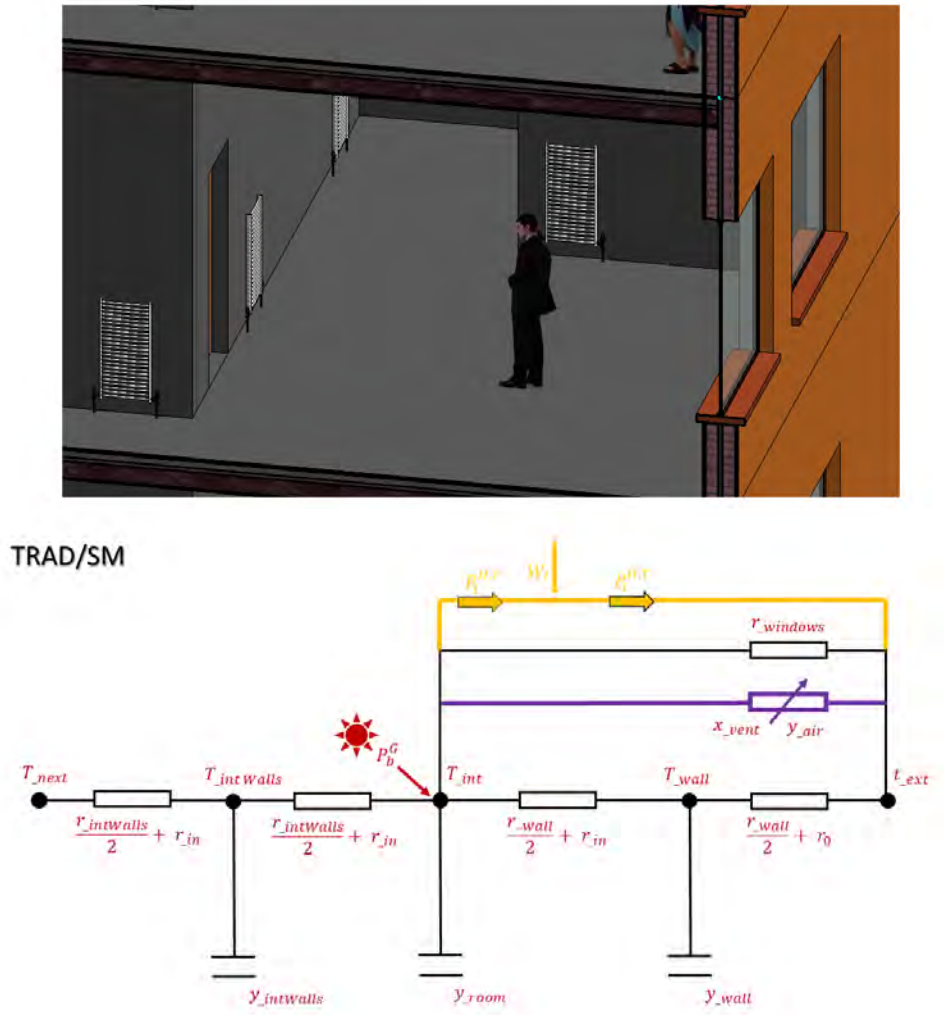

Figure 2: RC circuit for TRAD and SM units.

Case Study 1: EMS to minimize heating energy and cost. Our first case study compares the energy behavior of an apartment without (TRAD) and with (SM) EMS. The OF acts as a simulator for TRAD: it outputs the hourly heating demand required to maintain thermal comfort, and the room temperature is constant. For SM, the OF is an energy or cost minimizer, depending on the user's preference. The temperature varies in these minimizations. We present the results as a set of four graphs for each scenario (Figs. 3, 4, and 6). The first shows the amount of solar energy entering the unit, which is the sum of parameters $q_{i,g}^{sol,B}$ and $q_{i,g}^{sol,D}$. In our winter scenario, this helps to warm the unit. The second shows the temperatures outside, in the room, on the south-oriented wall, and on the internal walls. The third specifies the heating of the apartment: the dotted curve is

the HP output (corresponding to the demand), and the solid curve is the HP input. The fourth shows the ventilation flow between the room and the outside.

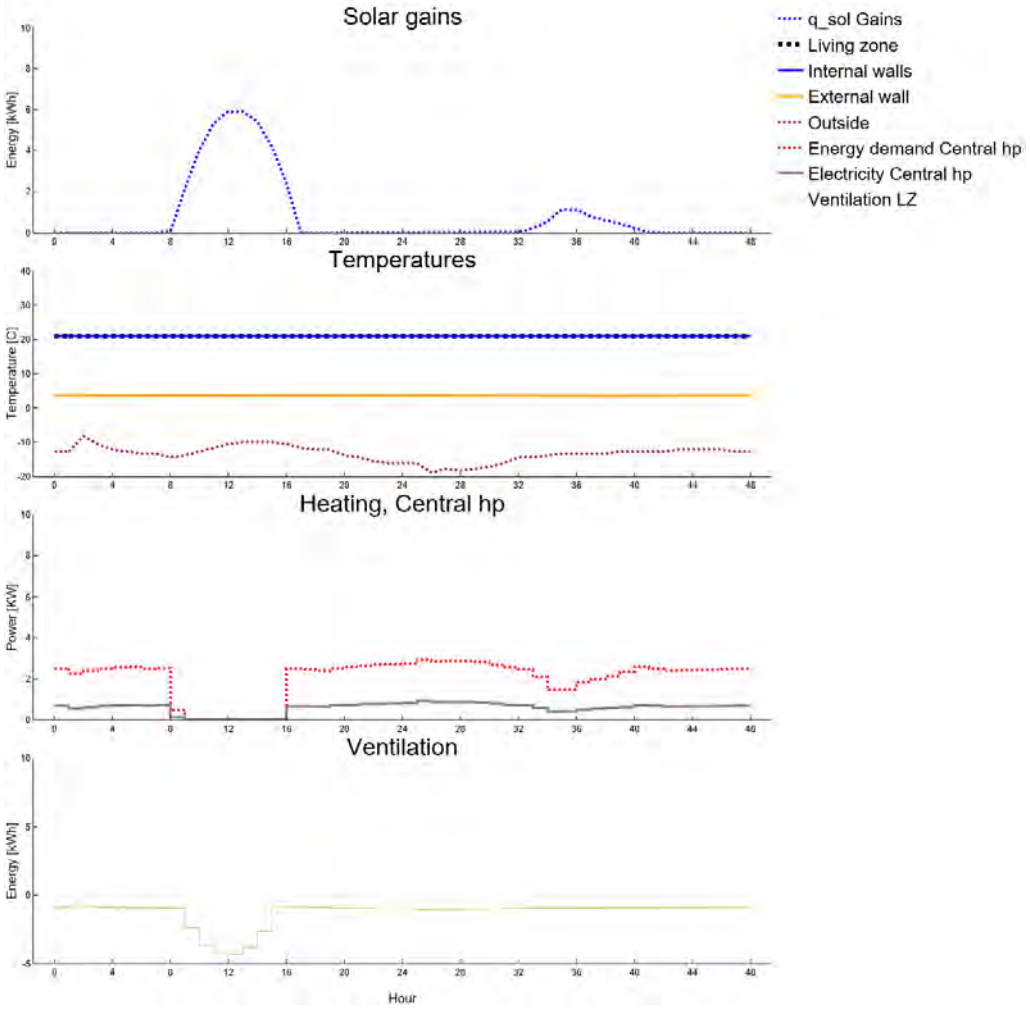

Figure 3: OF as simulator:
TRAD unit, South, Winter.

Figure 3 shows the energy behavior of TRAD; Fig. 4 shows the optimal demand for SM with the minimize-energy objective; and Fig. 6 shows the optimal demand for SM with the minimize-cost objective.

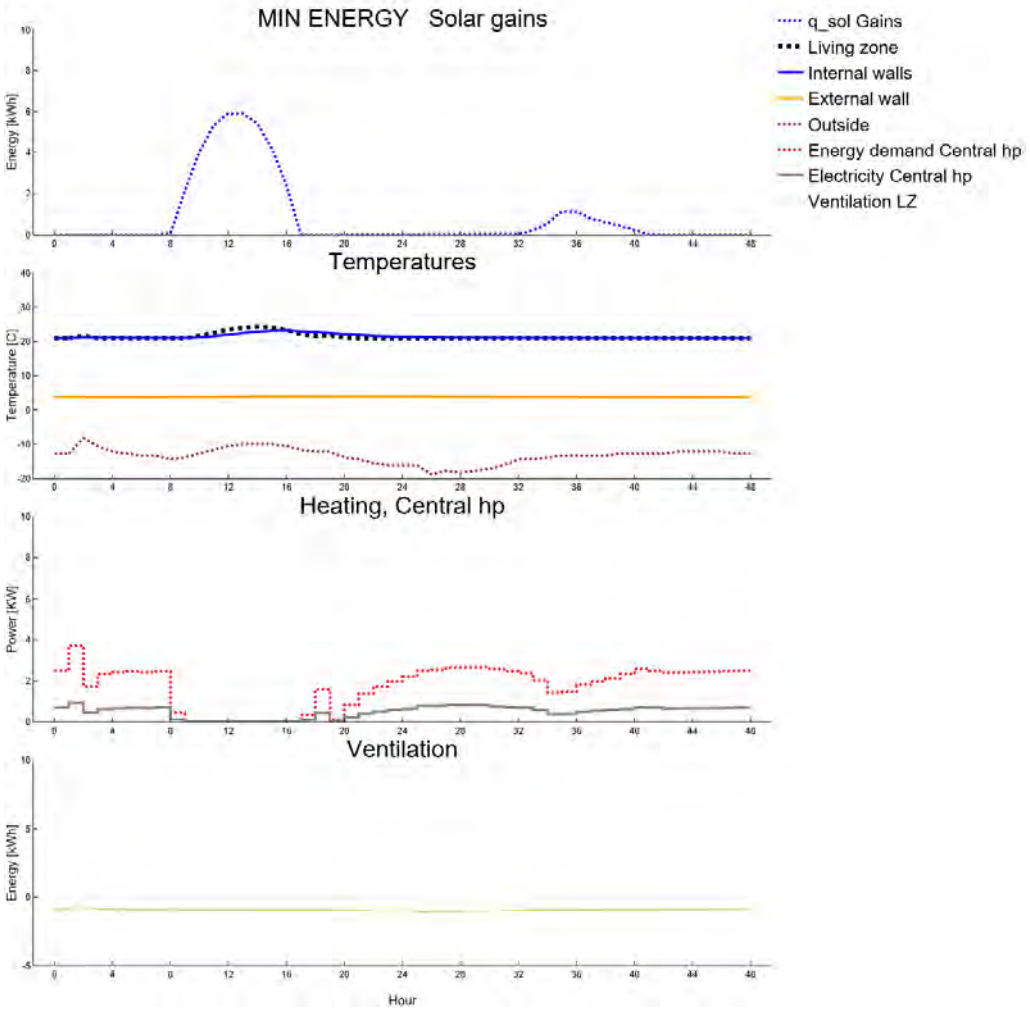

Figure 4: OF as simulator and optimizer:
SM unit, South, Winter, energy minimization.

First, we discuss the use of the OF as an EMS to minimize the energy consumption. It decreases the energy consumed by 14%: the total demand over the two days is 24 kWh instead of 28 kWh. It reduces the final cost too: SM is 15% cheaper than TRAD (2.02 CAD instead of 2.39 CAD).

Comparing Figs. 3 and 4, we make two observations. First, TRAD loses significant energy via ventilation. This happens during the solar-gain peaks, especially in the first day. TRAD keeps the room temperature constant, releasing surplus heat to the outside to avoid overheating. It then must buy energy during the subsequent hours. In contrast, SM stores surplus heat from sun radiation and uses it later. Second, SM buys more energy when E_l is higher, by allowing the indoor temperature to vary. The third plot in Fig. 4 shows this. The efficiency of the heat pump (E_l) depends on the input and

output temperature curves: the higher the gap, the lower the E_l. The beginning of day 1 is an example. During period 2 the temperature gap between the outside and the LZ is smaller than in period 3 (second plot). The EMS thus decides to buy around 4 kWh in period 2 (third plot).

Next, we discuss the EMS as a cost minimizer, using the tariff structure shown in Fig. 5. The EMS reduces the heating cost by 26%, from 2.39 CAD (TRAD) to 1.77 CAD (SM). It also reduces the total energy consumption by 7%, from 28 kWh to 26 kWh.

Figure 5 helps us to understand the optimization strategy. The tariff has three levels: low, medium, and high. The third plot in Fig. 6 shows that SM avoids buying energy during high-tariff and (to some extent) medium-tariff periods. It stores energy during the last low-tariff hours and uses that energy later in the day. However, the EMS also takes into account the efficiency of the heat pump. The unit buys electricity when the solar and internal gains do not keep the internal temperature in the comfort range. It buys more when E_l is higher: when the external temperature (brown dotted curve in temperature graph) and the room temperature (black dotted curve) are closer and the gap between the HP's output and input curves (respectively the red dotted and grey solid lines in the third graph) is larger. For instance, in time frames 0 to 4 there are no solar gains and the unit buys electricity. It buys more in periods 1 and 2, when the external temperature is warmer and the HP efficiency is higher.

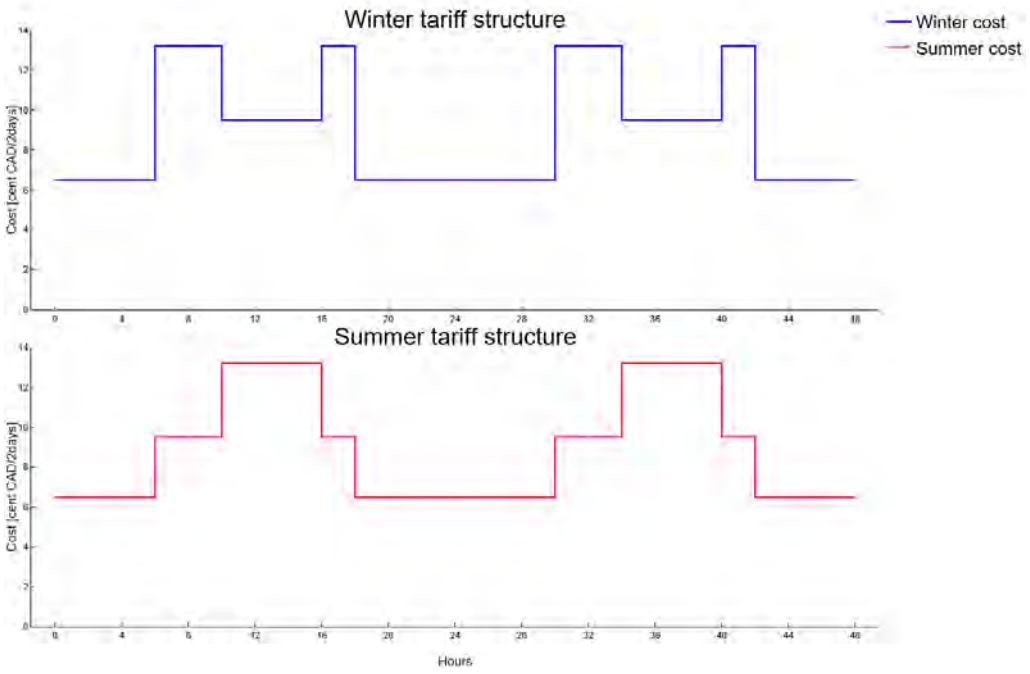

Figure 5: Tariff structure: Ontario TOU.

The EMS cost minimizer achieves an important cost reduction, but it increases the power fluctuation. SM requires up to 7 kW, whereas TRAD never exceeds 2.5 kW. This may be an issue for the operator. In contrast, when the EMS is used as an energy

minimizer, the power peaks are lower than for TRAD and the cost minimizer, and they rise only when the external temperature is higher. In other words, the energy minimizer reduces the overall energy demand and shifts the power peaks from high-demand to low-demand hours.

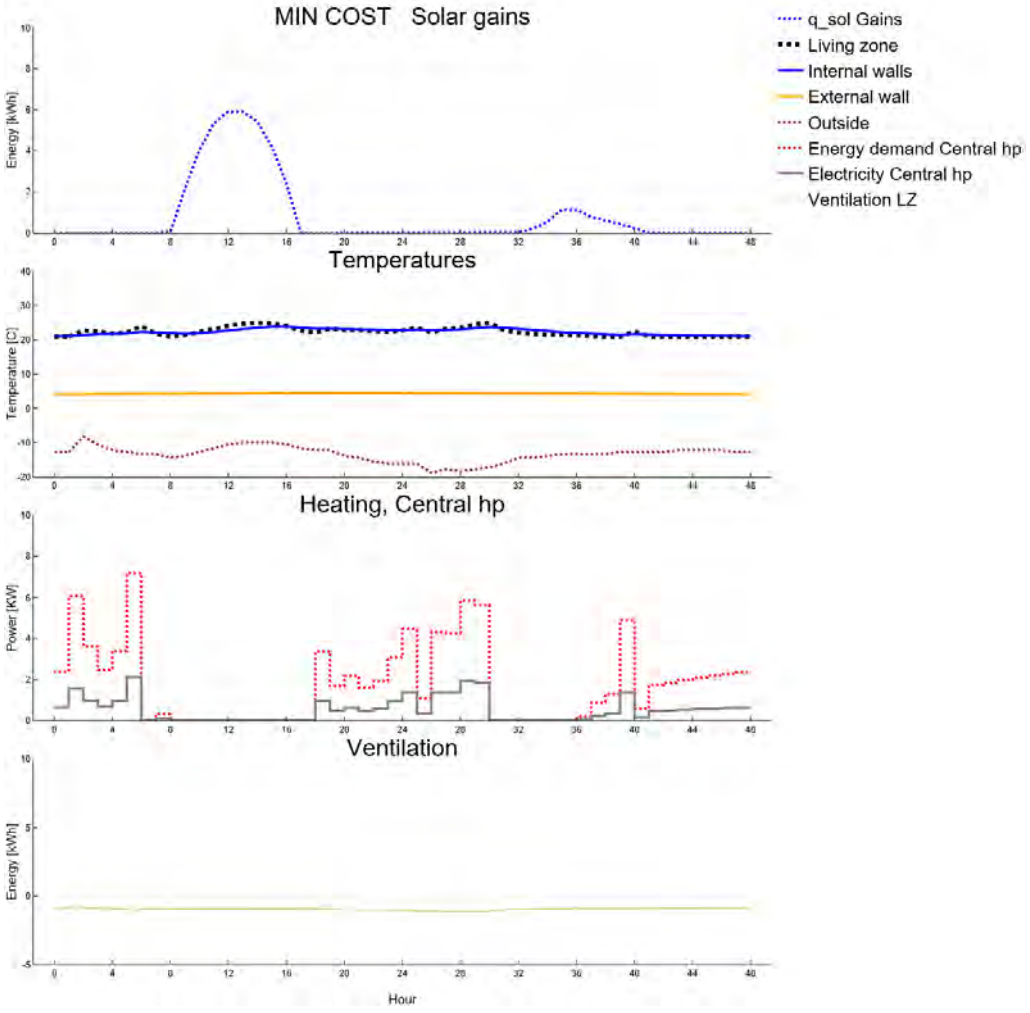

Figure 6: OF as simulator and optimizer:
SM unit, South, Winter, cost minimization.

Further comparing the two SM cases, we see that the temperature varies more when the EMS minimizes cost. This is because it must follow both the tariff structure and the HP's E_l.

The following table summarizes the cost and energy consumption of the three cases, with the percentage reductions achieved by the SM cases given in parentheses.

	TRAD	SM energy-min	SM cost-min
Total cost [CAD/2days]	2.39	2.02 (15%)	1.77 (26%)
Total energy [kWh/2days]	28	24 (14%)	26 (7%)

5.2. Building design

In this section we discuss the impact of the building design. We test the OF with a standard external wall and a DSF with dynamic solar shading, and we minimize the cost. We apply the EMS applied to the SM unit of the previous section and then to the same unit with the addition of a smart dynamic façade (the DYN unit).

Standard façade vs. DSF with smart shading. The SM unit has the traditional external wall, the layers of which are given in the following table. The parameters r_0 and r_{in} refer to EN ISO 13786: they are external and internal heat-transfer resistance values.

Standard façade thermal features

Layer name	thermal conductivity [W/m K]	gross density [kg/m^3]	specific heat capacity [j/kg K]	layer thickness [m]	R [m^2 K/W]
r_{in}					0.13
Gypsum	0.16	801	840	0.02	0.125
Insulation	0.03	28.8	1210	0.12	4
Air	0.04	1.2	1000	0.07	1.75
Brick	1.31	2082.6	920	0.10	0.076
r_0					0.04

U-value [W/m^2 K]	Total thickness [m]
0.16	0.31

The smart façade of the DYN unit has three elements: the external wall, an air gap with dynamic shading, and an external glass skin. Figure 7 shows the RC circuit, and the table below lists the thermal features of the DSF.

Thermal features of double skin façade

Layer name	thermal conductivity [W/m K]	gross density [kg/m^3]	specific heat capacity [j/kg K]	layer thickness [m]	R [m^2 K/W]
Rsi					0.13
Gypsum	0.16	801	840	0.02	0.125
Insulation	0.03	28.8	1210	0.12	4
Air	0.04	1.2	1000	0.07	1.75
Brick	1.31	2082.6	920	0.10	0.076
Rsi					0.13
Air	0.04	1.2	1000	0.80	20
Glass	0.04	2500	792	0.02	0.56
Rse					0.04

U-value [W/m^2 K]	Total thickness [m]]
0.03	1.13

DYN has a more complex ventilation system than SM. There are three ventilation flows (purple lines in Fig. 7): between the LZ and the DSF air cavity; the air cavity and the exterior; and the LZ and the exterior.

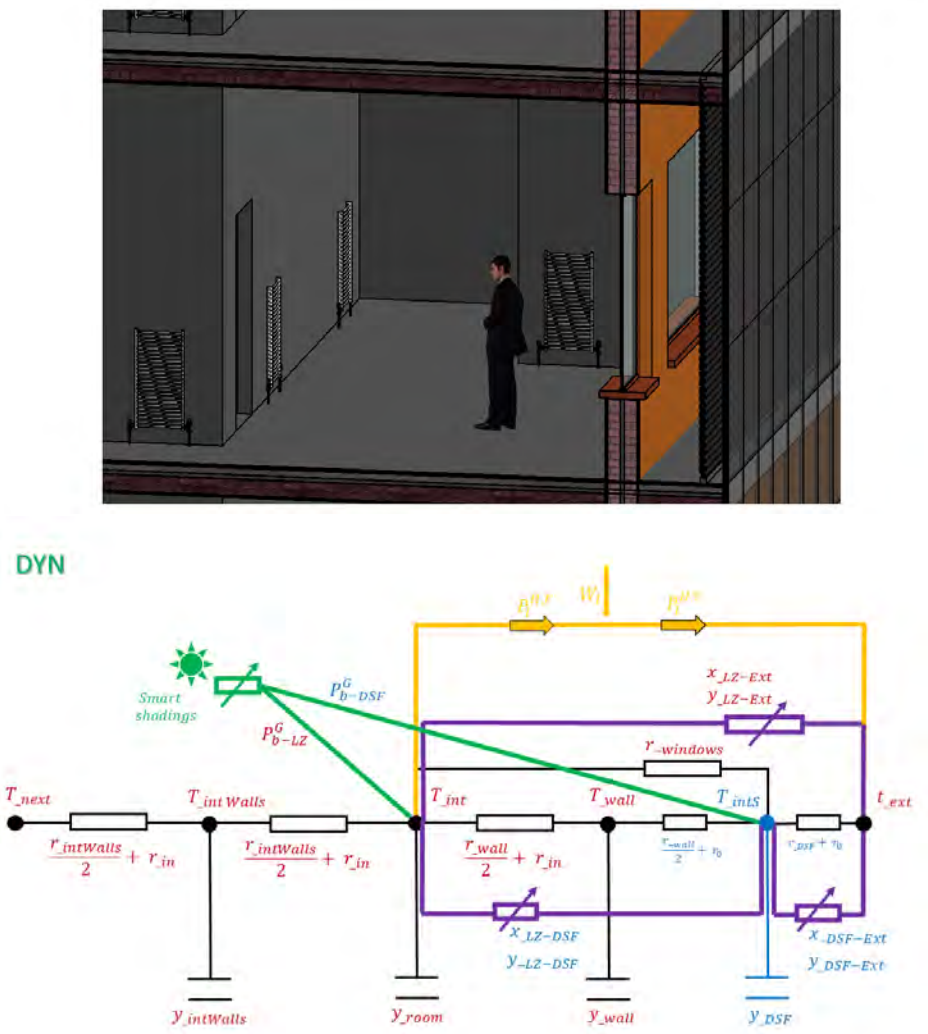

Figure 7: RC circuit for DYN unit.

The dynamic shading and ventilation are controlled by the EMS. The smart shading is represented in green in Fig. 7. The EMS chooses its configuration according to the optimal amount of solar radiation (9). The smart shading manages the solar energy entering the room, which is a form of local renewable energy generation. The temperature inside the air cavity depends on its heat capacity, so the DYN model has one more node in the circuit. Power flows into this node: it represents local energy generation and is

indicated by P^{G}_{g-DSF} in Fig. 7, where the elements specific to DYN are shown in blue.

Case Study 2. Our second case study compares the SM unit and the DYN unit, with cost minimization. We consider a south-oriented apartment during two winter days. Fig. 6 above gives the SM results, and Fig. 8 gives the DM results.

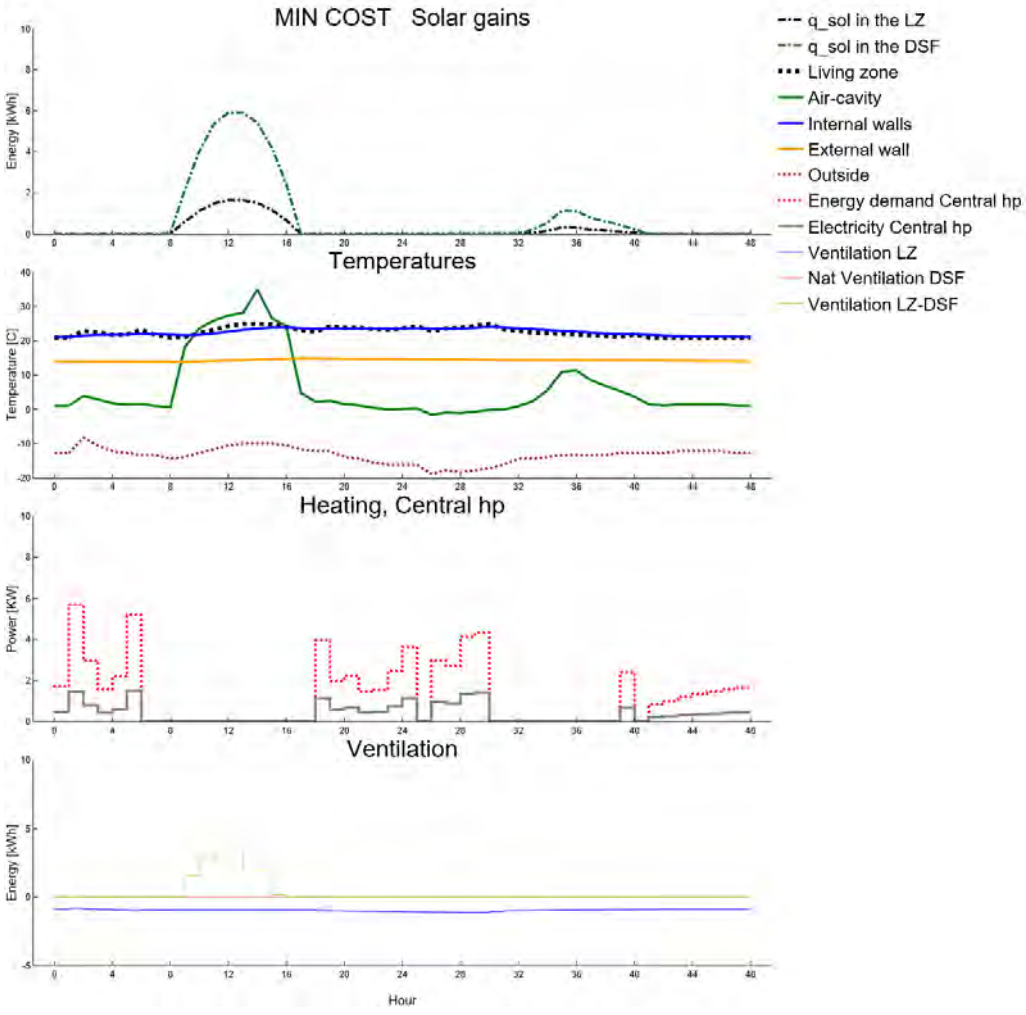

Figure 8: OF to double skin façade:
DYN unit, South, Winter, cost minimization.

The DYN unit has three advantages. First, it is better insulated because of the DSF. Thus, it has lower thermal losses, lower energy consumption, smaller power peaks before the high-tariff period, and improved indoor comfort. Second, DYN has a larger thermal storage capacity, so it can more readily adjust to electricity cost and weather variations and is thus cheaper than SM. Third, the dynamic shading allows more efficient control over the local energy generation, giving a further cost reduction.

DYN captures and stores solar energy in two physical spaces. Solar gains first enter the air cavity of the DSF (green line in the first graph of Fig. 8), where part of their energy is stored. They then reach the LZ, passing through the windows of the inner skin (black line in graph of Fig. 8).

The solar gain entering the unit is controlled by the variable Δ_i, represented in the second graph (Fig. 8). $\Delta_{i,b}$ can vary within a range chosen by the user (see Equation 10). We want to ensure sufficient natural light in the LZ, so we allow Δ to range from 0.3 to 1, where $\Delta_i = 1$ means that the shades are fully open. The lower bound ensures adequate visual comfort (see [33]). In winter, it is optimal to capture as much solar energy as possible, so $\Delta_{i,b}$ is 1 during the solar-gain hours (Fig. 8). In summer, $\Delta_{i,b}$ significantly impacts the energy demand of the unit.

The third graph of Fig. 8 shows first that the indoor temperature (black curve) fluctuates less in DYN than SM. Second, the external wall (orange curve) is warmer and, because of its large thermal inertia, helps to reduce the overall thermal loss. Third, during some solar-gain hours, the DSF temperature (green curve) is higher than that indoors. When this happens, the thermal losses turn into gains. Consequently, the EMS activates ventilation between the LZ and the air cavity, as the final plot shows. This warm air helps to heat the room, reducing the use of the HP (fourth plot in Fig. 8).

The fourth plot shows that the EMS affects the electricity demand of DYN in three ways. First, it lowers the power peaks: they are always below 6 kW (SM reaches 7 kW). Second, it expands the time window during which the heating system is off. Because of its large thermal inertia and improved insulation, DYN is less dependent on the grid and more attractive for DR purposes. Third, it reduces the overall energy consumption.

To summarize, DYN is cheaper than both SM and TRAD. Furthermore, it requires less energy and reduces the power peaks. The following table shows the cost and energy consumption of the two scenarios. The percentage reductions are given in parentheses.

	TRAD	Standard façade	DSF with dynamic shading
Total cost [CAD/2days]	2.39	1.77 (26%)	1.23 (49%)
Total energy [kWh/2days]	28	26 (7%)	18.3 (35%)

5.3. Unit orientation

In this section we discuss the impact of the unit orientation and the potential for DR. We consider four TRAD units and four DYN units with different orientations. We study two days with the summer tariff of Ontario, Canada (Fig. 5), and we compare the results.

Case Study 3. The following table shows that the DYN units are about 96% cheaper than the TRAD units. Furthermore, the DYN units have a lower energy demand; this is because of the EMS operations and their smart design.

Figures 9 to 13 show two interesting aspects of the shading and cooling operations. First, the smart shading in the DYN units automatically reduces the solar gains in summer days so as to reduce the need for cooling, but allows the full solar gain in the winter days where its heating effect reduces the need for other heating. The EMS minimizes the cooling loads, which are closely connected to the solar gains and the orientation. Second, the EMS uses the structure of the DYN units as cold storage: it cools the unit during the night (by running the central heat pump or by ventilating) and

releases the indoor heat during the day. During day 1, when the exterior temperature is lower than that indoors, the EMS avoids buying electricity and relies on ventilation. During day 2 it turns on the HP but only during off-peak hours.

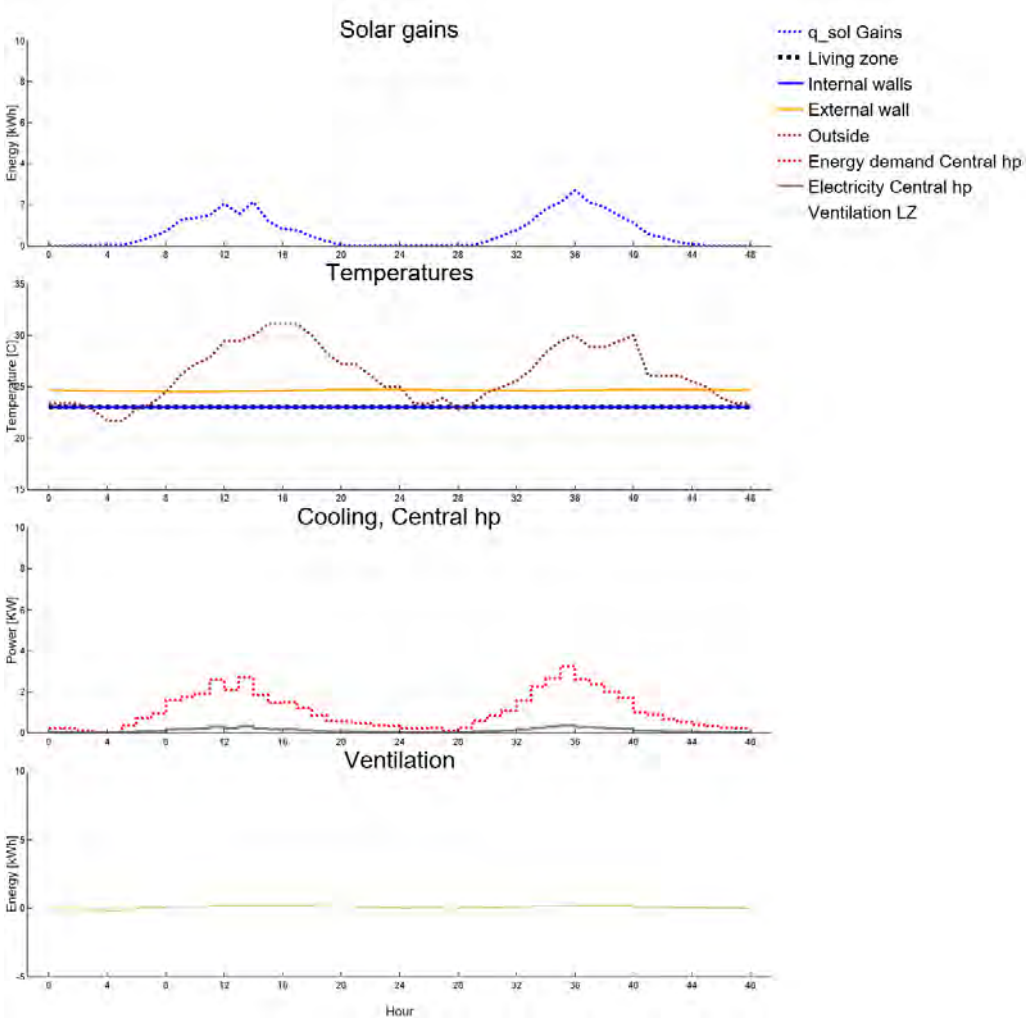

Figure 9: OF as simulator:
TRAD unit, South, Summer.

The results show the importance of orientation: the units have different energy requirements and the EMS strategy adapts accordingly. The east and west units have the highest cooling demand. The west unit captures solar energy until late in the afternoon and so stays warm longer. Consequently, on day 2, the west unit turns on the HP one hour earlier than the other orientations do. The TRAD units' cooling demand mainly depends on the solar-gain peaks (Fig. 9). On the other hand, the DYN demand depends on the tariff structure and the HP E_l.

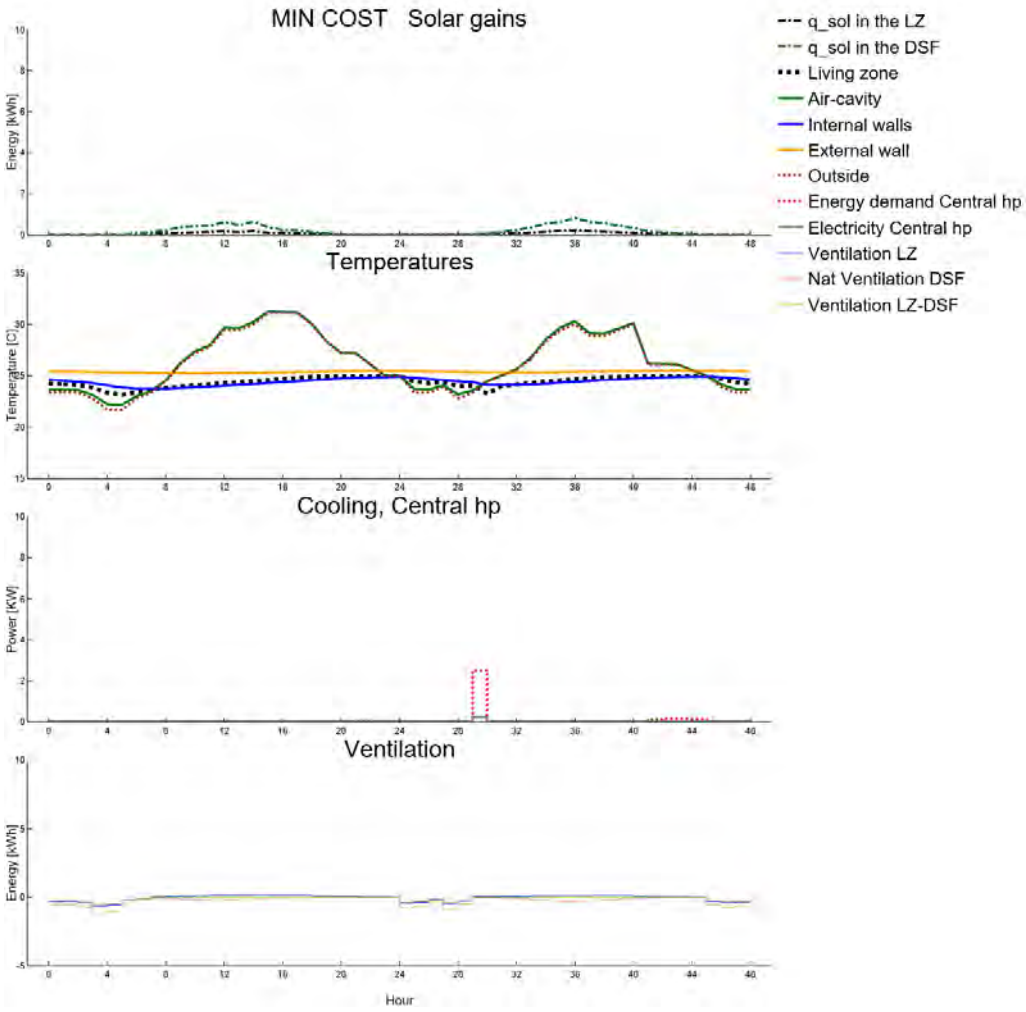

Figure 10: OF as cost minimizer:
DYN unit, South, Summer.

OF applied to TRAD and DYN for different orientations

	TRAD		DYN		% reduction for DYN
	[CAD/2days]	[kWh/2days]	[CAD/2days]	[kWh/2days]	
South	0.64	5.7	0.021	0.39	97%
East	0.66	6.35	0.025	0.38	96%
West	0.76	7.11	0.032	0.46	96%
North	0.49	4.66	0.016	0.24	97%

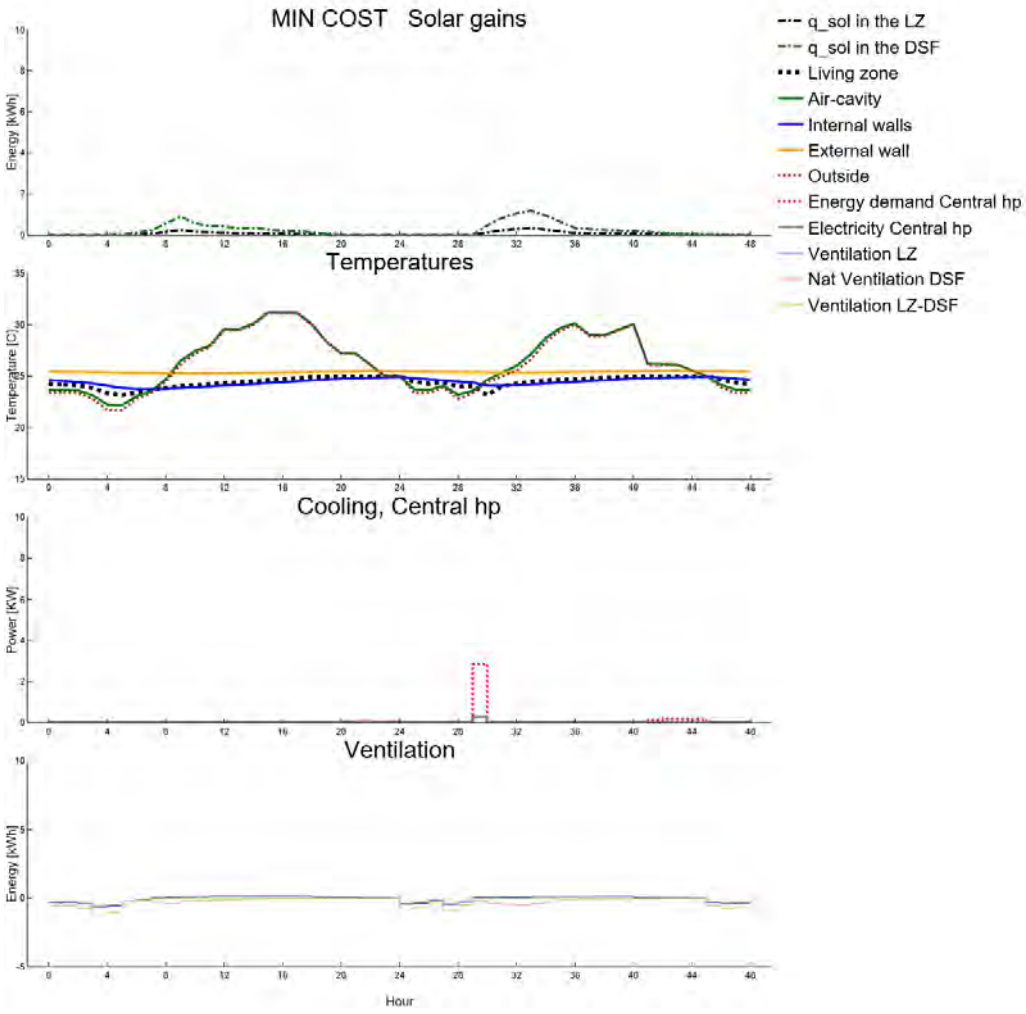

Figure 11: OF as cost minimizer:
DYN unit, East, Summer.

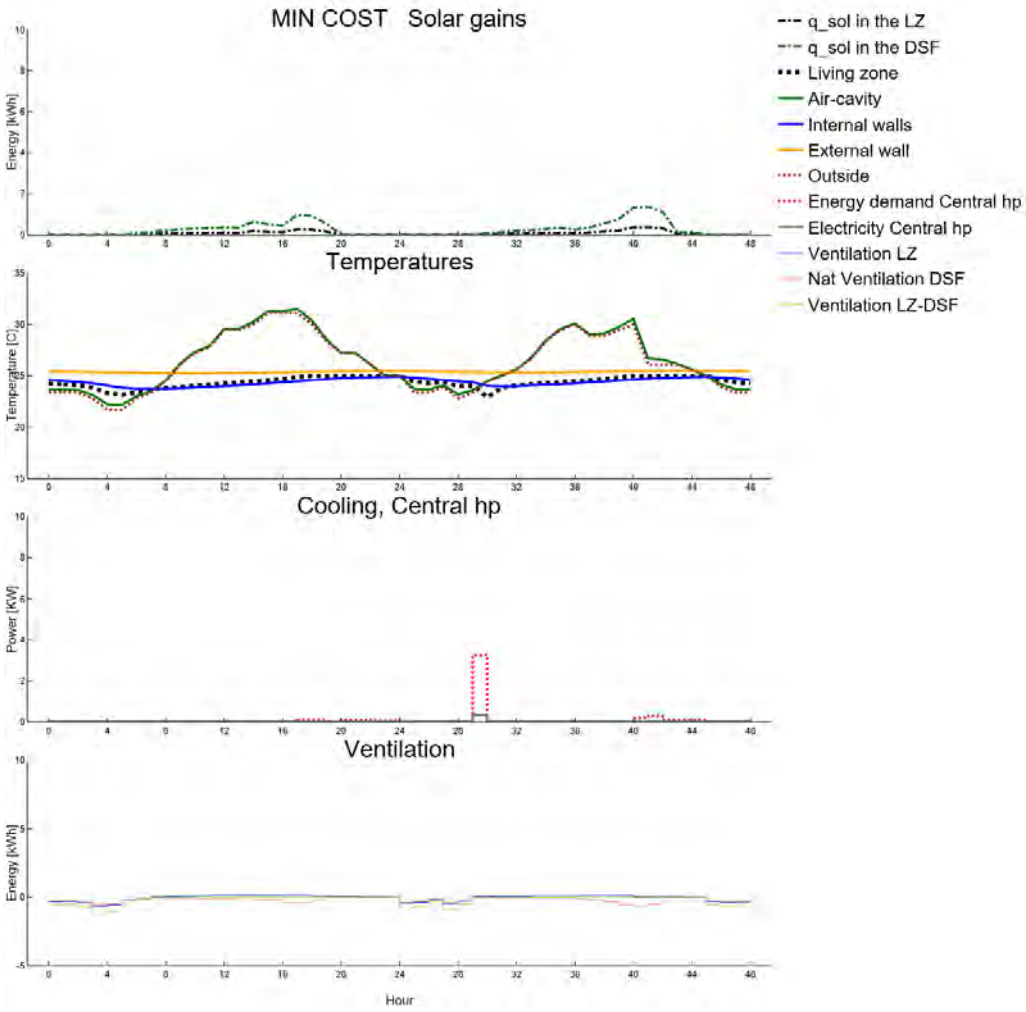

Figure 12: OF as cost minimizer:
DYN unit, West, Summer.

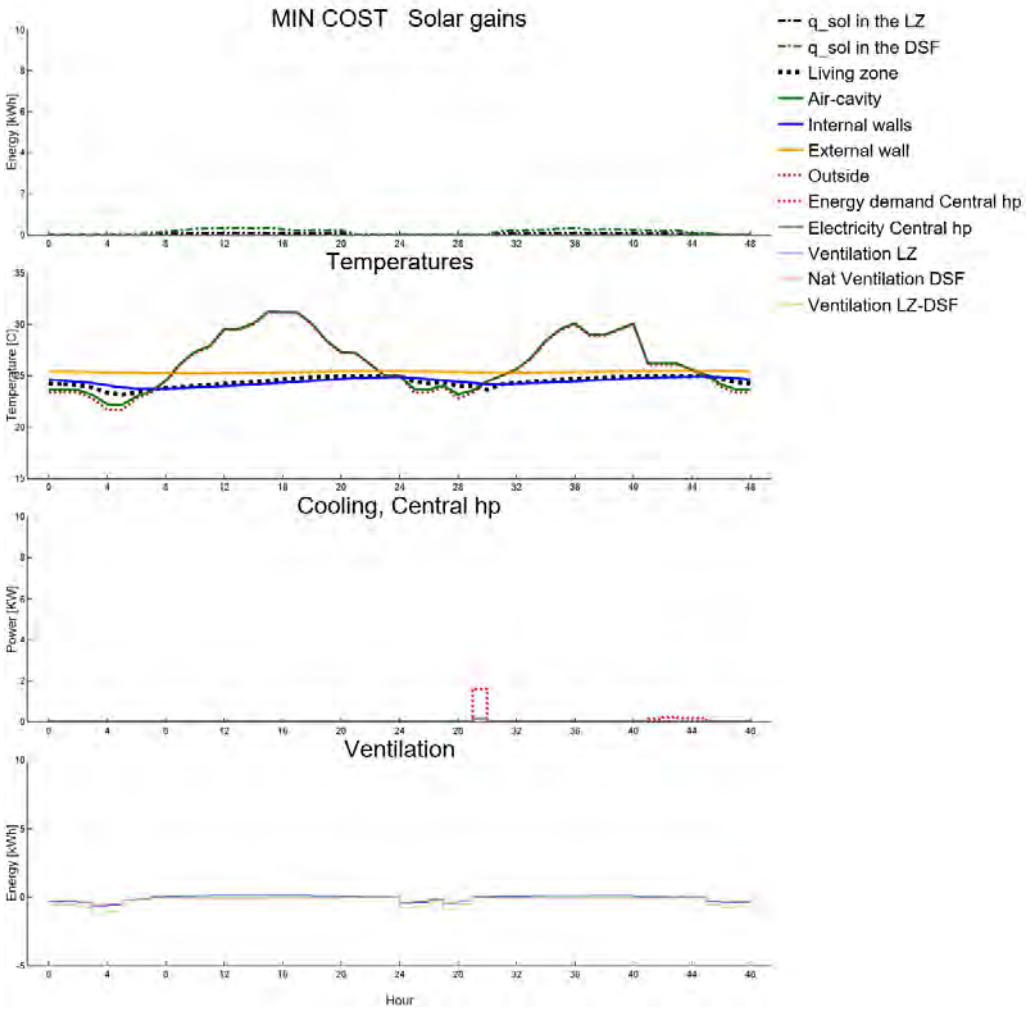

Figure 13: OF as cost minimizer:
DYN unit, North, Summer.

5.4. Heating system configuration

In this section we discuss the impact of the HP location. In case 1, we consider a central HP that works between the exterior and interior. In this scenario the building heating is centralized. In case 2, the apartment has two HPs: one central and one local. The local HP is located in the DSF air cavity and it operates between the DSF and the interior. We simulate a south-oriented unit on two winter days, and we minimize the energy. For each case, we consider a) the solar gains of the previous simulations, and b) scaled solar gains.

Case Study 4. The first set of results shows the optimal behaviour for the original solar gain profile with the central heat pump only (Fig. 14) and the behaviour with both

central and local heat pumps (Fig. 15). It mainly benefits from ventilation between the air cavity and the LZ. It warms the room before the solar peak hours to increase the temperature of the DSF, and it then uses solar energy to make the air cavity temperature higher than that of the LZ. When the DSF is warmer than the room, the EMS heats up the apartment by natural ventilation. In case 2, the EMS uses the local HP during the solar-gain hours (Fig. 15). The local HP is at its most efficient during these hours.

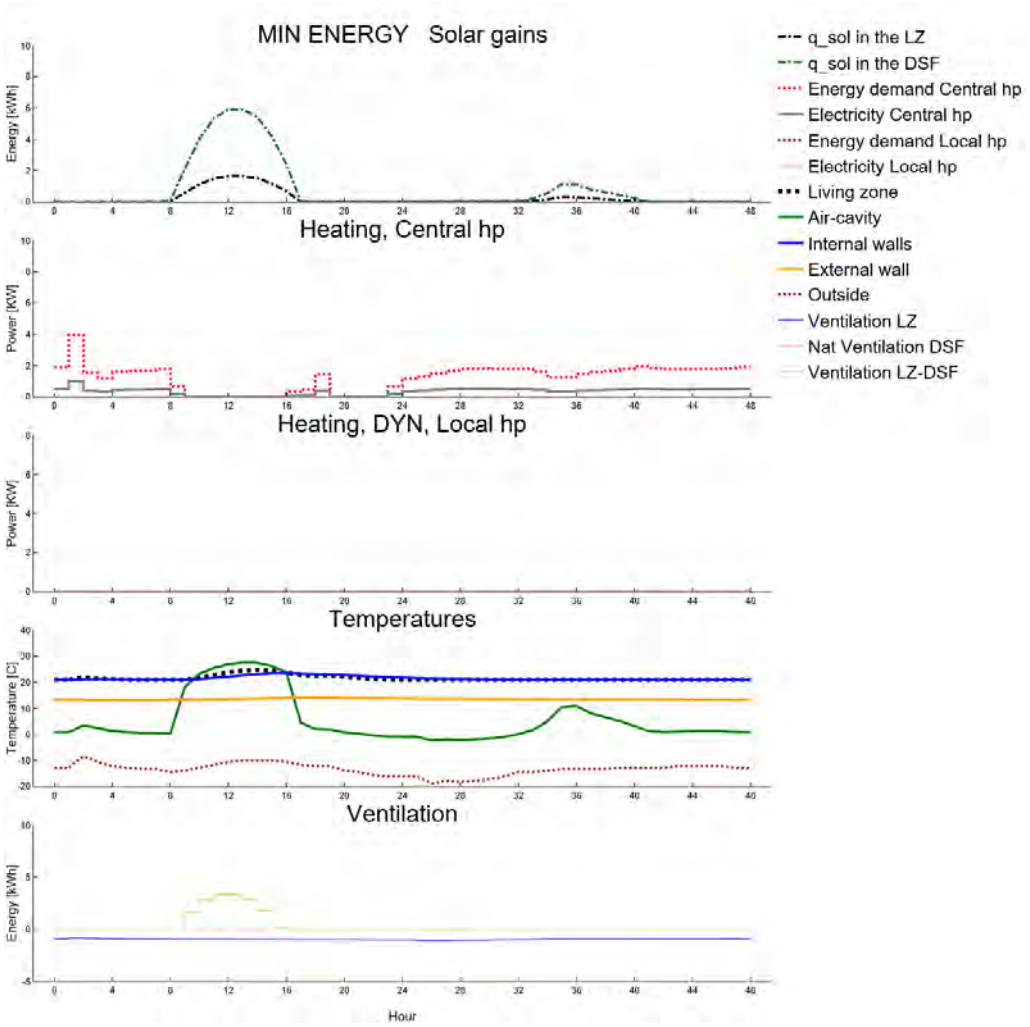

Figure 14: Case 1a: OF as cost energy minimizer: DYN unit, South, Winter. Central heat pump, Original solar profile.

There is a small difference between the heating demand of cases 1 and 2. In case 1, the total energy consumption is 16.60 kWh and in case 2 it is 16.43. This is due in part to the high efficiency of the two HPs and in part to the weather conditions.

The second set of results shows that the value of a local HP depends on the solar

gains. In these results (Figs. 16 and 17), we scale the solar gains on day 1 and day 2 by 0.35 and 1.90, respectively. The solar gains are no longer sufficient to raise the air cavity temperature above that of the room. The EMS can not benefit from natural ventilation and must turn on the HP.

In case 2b (Fig. 17), the optimal solution is to run the local HP during the midday hours, when the DSF is warmer than the exterior. The EMS takes advantage of the high E_l of the local HP: its value at these times is about 7.5, whereas E_l for the central heat pump at these times about 3.8. The magnitude of the E_l of a HP is the ratio of the values of the curves of energy demand (dotted line) and electricity (solid) of heat pump graphs.

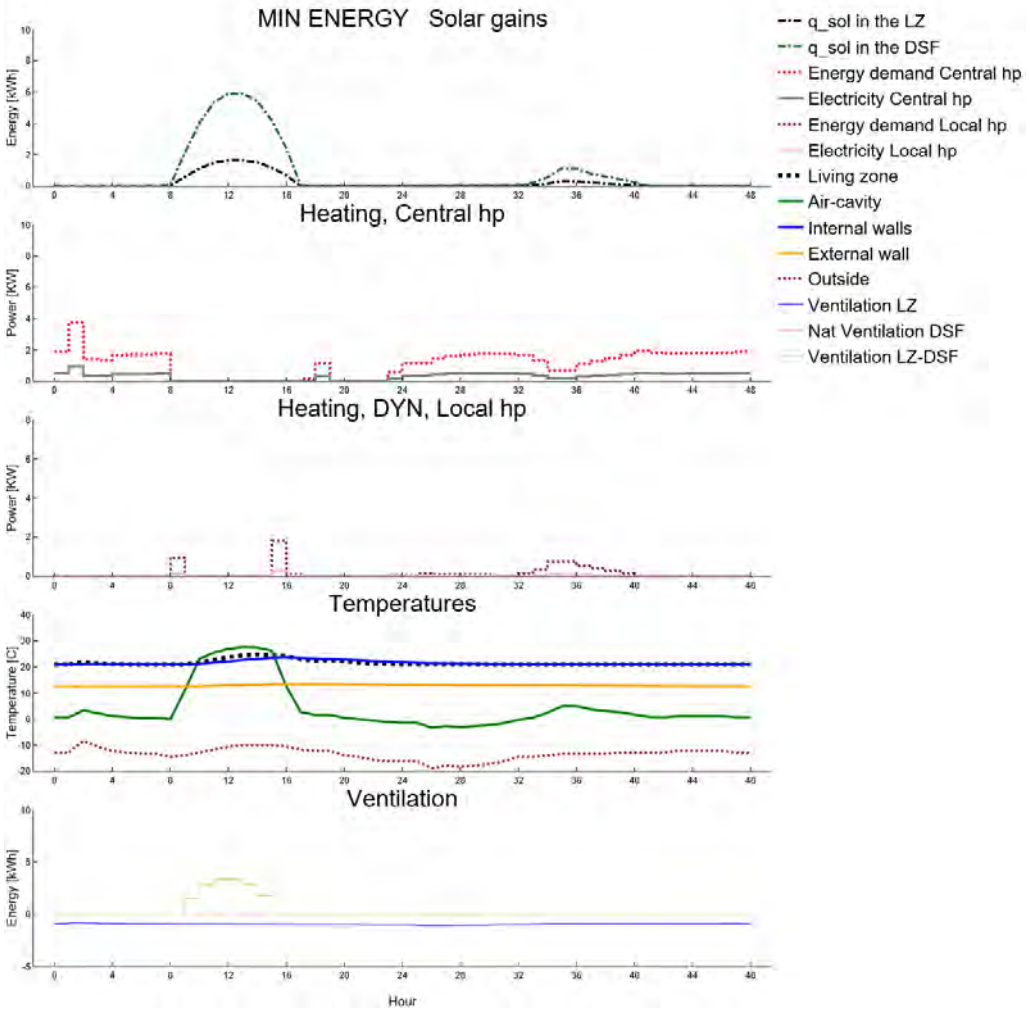

Figure 15: Results for case 2a: DYN unit, South, Winter, Energy min, 2 heat pumps.

When the local HP is running, the temperature of the DFS drops, causing heat flows

between the unit and the environment. Thus, over-use of the local HP will lead to an excessively low DSF temperature that may increase the thermal loss from the room.

The following table summarizes the two sets of results.

Case	Assumptions		Results		
	Solar gains day 1	Solar gains day 2	Total energy [kWh/2days]	Final cost [CAD/2days]	Strategy
1a	$q_{i,s}^{sol}$	$q_{i,s}^{sol}$	16.60	1.45	HP + ventilation
2a	$q_{i,s}^{sol}$	$q_{i,s}^{sol}$	16.43	1.43	2 HPs + ventilation
1b	$0.35q_{i,s}^{sol}$	$1.9q_{i,s}^{sol}$	24.68	1.64	HP
2b	$0.35q_{i,s}^{sol}$	$1.9q_{i,s}^{sol}$	23.94	1.61	2 HPs

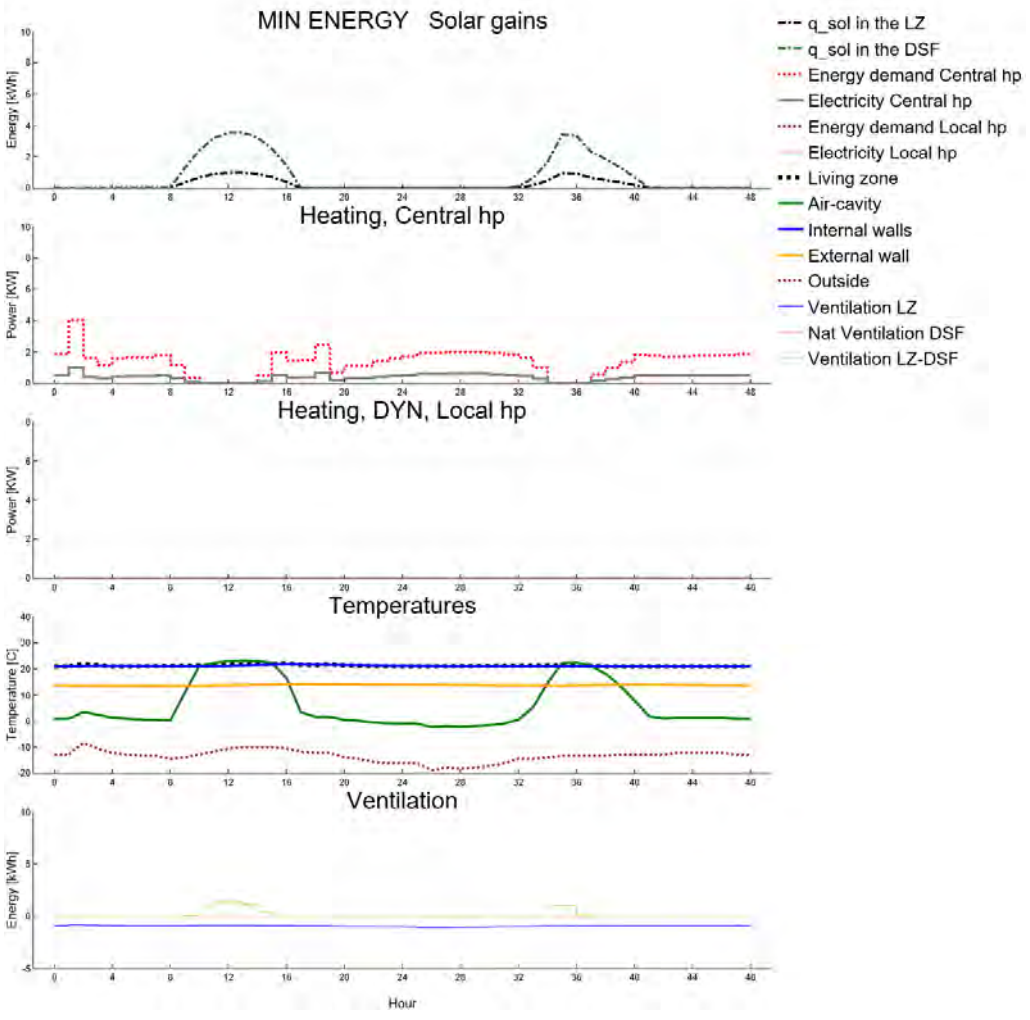

Figure 16: Results for case 1b: DYN unit, South, Winter, Energy min, central heat pump.

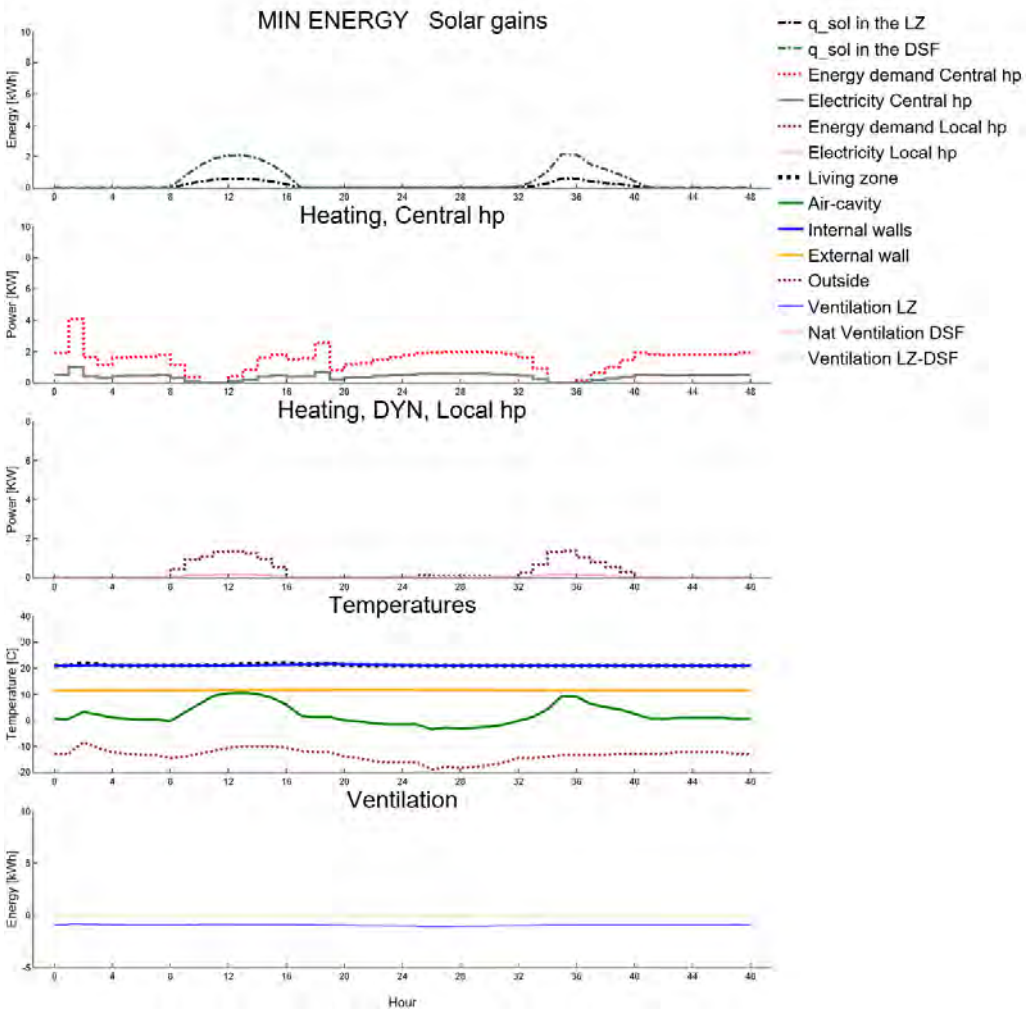

Figure 17: Results for case 2b: DYN unit, South, Winter, Energy min, 2 heat pumps.

6. Conclusion and Future Research

We have proposed an optimization-based DSM system for smart buildings (EMS). The optimization problem is a nonlinear programming model that is solved by off-the-shelf solvers. The use of this DSM system allows the unit to reduce heating and cooling consumption during predefined hours by encouraging the consumers to shift load. We provided insight into how combining optimization with the building features not only facilitates this load shifting but also helps to reduce the overall heating and cooling demand.

We demonstrated the use of the DSM system in different situations. First, we applied the EMS to minimizing the heating consumption and cost. When we minimized energy, the EMS reduced the heating consumption by 14%. When we minimized cost, it lowered

the electricity cost by 26%. Second, we considered a unit with a traditional external wall and the same unit with a DSF. The EMS reduced both the heating consumption and the final electricity cost. The consumption and cost for the DSF unit decreased by 35% and 49% respectively. Third, we applied the EMS to four units with different orientations, reducing their electricity cost by up to 97%. Fourth, we applied the EMS to a unit with a single central HP and to one with two HPs, one central and one local (within the DSF). The latter unit achieved a small energy reduction.

Future work could use the OF as a tool to help design the best DR strategy. First, it may be of interest to model longer off-peak time windows, to lower the power peaks. Second, the OF could be used to avoid a situation where all the users wish to buy electricity in the same time period: a carefully designed personalized tariff for each user could spread such purchases over multiple periods. Future work will also include the application of the approach to larger instances such as heat districts, and the consideration of heat-recovery and energy sharing systems.

Acknowledgments

This research was supported by the Canadian NSERC Energy Storage Technology (NEST) Network.

References

[1] PowerShift Atlantic. Final Report For Clean Energy Fund (CEF), 2015. `https://www.nbpower.com/media/1489367/nb_power_psa_en_outreach_report.pdf`, accessed 2020-04-26.

[2] Adham I Tammam, Miguel F. Anjos, and Michel Gendreau. Balancing supply and demand in the presence of renewable generation via demand response for electric water heaters. *Annals of Operations Research*, Online First 31 March 2020.

[3] F Malandra, AC Kizilkale, F Sirois, B Sansò, MF Anjos, M Bernier, M Gendreau, and RP Malhamé. Smart Distributed Energy Storage Controller (smartDESC). *Energy*, 210:118500, 2020.

[4] Diana Urge-Vorsatz, Luisa F Cabeza, Susana Serrano, Camila Barreneche, and Ksenia Petrichenko. Heating and cooling energy trends and drivers in buildings. *Renewable and Sustainable Energy Reviews*, 41:85–98, 2015.

[5] California Public Utilities Commission. Consumer FAQ on DR Providers (also known as Aggregators), 2020. `https://www.cpuc.ca.gov/General.aspx?id=6306`, accessed 2020-04-26.

[6] Samuel F Fux, Araz Ashouri, Michael J Benz, and Lino Guzzella. EKF based self-adaptive thermal model for a passive house. *Energy and Buildings*, 68:811–817, 2014.

[7] Miguel F Anjos and Juan A Gómez. Operations research approaches for building demand response in a smart grid. In *Leading Developments from INFORMS Communities*, pages 131–152. INFORMS, 2017.

[8] Juan A Gomez-Herrera and Miguel F Anjos. Optimal collaborative demand-response planner for smart residential buildings. *Energy*, 161:370–380, 2018.

[9] Berk Celik, Robin Roche, Siddharth Suryanarayanan, David Bouquain, and Abdellatif Miraoui. Electric energy management in residential areas through coordination of multiple smart homes. *Renewable and Sustainable Energy Reviews*, 80:260–275, 2017.

[10] Yuanguo Zhu. Optimal control for multistage uncertain systems. In *Uncertain Optimal Control*, pages 69–97. Springer, 2019.

[11] E. Kuznetsova and M. F. Anjos. Challenges in energy policies for the economic integration of prosumers in electric energy systems: A critical survey with a focus on Ontario (Canada). *Energy Policy*, 142, 2020.

[12] Rehman Zafar, Anzar Mahmood, Sohail Razzaq, Wamiq Ali, Usman Naeem, and Khurram Shehzad. Prosumer based energy management and sharing in smart grid. *Renewable and Sustainable Energy Reviews*, 82:1675–1684, 2018.

[13] Rosemarie Velik and Pascal Nicolay. Energy management in storage-augmented, grid-connected prosumer buildings and neighborhoods using a modified simulated annealing optimization. *Computers & Operations Research*, 66:248–257, 2016.

[14] José Iria and Filipe Soares. A cluster-based optimization approach to support the participation of an aggregator of a larger number of prosumers in the day-ahead energy market. *Electric Power Systems Research*, 168:324–335, 2019.

[15] Jennifer Date, José A Candanedo, Andreas K Athienitis, and Karine Lavigne. Predictive setpoint optimization of a commercial building subject to a winter demand penalty affecting 12 months of utility bills. *Building Simulation Conference, San Francisco*, 2017.

[16] Giuseppe Tommaso Costanzo, Guchuan Zhu, Miguel F. Anjos, and Gilles Savard. A system architecture for autonomous demand side load management in smart buildings. *IEEE Transactions on Smart Grid*, 3(4):2157–2165, 2012.

[17] Guruprasad Alva, Yaxue Lin, and Guiyin Fang. An overview of thermal energy storage systems. *Energy*, 144:341–378, 2018.

[18] R Parameshwaran, S Kalaiselvam, S Harikrishnan, and A Elayaperumal. Sustainable thermal energy storage technologies for buildings: A review. *Renewable and Sustainable Energy Reviews*, 16(5):2394–2433, 2012.

[19] Sebastian Stinner, Kristian Huchtemann, and Dirk Müller. Quantifying the operational flexibility of building energy systems with thermal energy storages. *Applied Energy*, 181:140–154, 2016.

[20] Lidia Navarro, Alvaro De Gracia, Shane Colclough, Maria Browne, Sarah J McCormack, Philip Griffiths, and Luisa F Cabeza. Thermal energy storage in building integrated thermal systems: A review. Part 1. active storage systems. *Renewable Energy*, 88:526–547, 2016.

[21] Marco Filippi and Enrico Fabrizio. Il concetto di zero energy building. *AICARR, Milano*, 2011.

[22] European Commission. Directive 2010/31/EU of the European Parliament and of the Council of 19 May 2010 on the energy performance of buildings (recast). *Official Journal of the European Union*, 18(06), 2010.

[23] Paul Moran, Jamie Goggins, and Magdalena Hajdukiewicz. Super-insulate or use renewable technology? Life cycle cost, energy and global warming potential analysis of nearly zero energy buildings (NZEB) in a temperate oceanic climate. *Energy and Buildings*, 139:590–607, 2017.

[24] Eike Musall. Net zero energy buildings - worldwide. `https://batchgeo.com/map/net-zero-energy-buildings`, 2013.

[25] Shane Colclough, Oliver Kinnane, Neil Hewitt, and Philip Griffiths. Investigation of NZEB social housing built to the passive house standard. *Energy and Buildings*, 179:344–359, 2018.

[26] Francesco Pomponi, Poorang AE Piroozfar, Ryan Southall, Philip Ashton, and Eric RP Farr. Energy performance of double-skin façades in temperate climates: A systematic review and meta-analysis. *Renewable and Sustainable Energy Reviews*, 54:1525–1536, 2016.

[27] J Darkwa, Y Li, and DHC Chow. Heat transfer and air movement behaviour in a double-skin façade. *Sustainable Cities and Society*, 10:130–139, 2014.

[28] Ali Ghaffarianhoseini, Amirhosein Ghaffarianhoseini, Umberto Berardi, John Tookey, Danny Hin Wa Li, and Shahab Kariminia. Exploring the advantages and challenges of double-skin façades (DSFs). *Renewable and Sustainable Energy Reviews*, 60:1052–1065, 2016.

[29] Francesco Pomponi, Poorang AE Piroozfar, Ryan Southall, Phil Ashton, and Eric RP Farr. Life cycle energy and carbon assessment of double skin façades for office refurbishments. *Energy and Buildings*, 109:143–156, 2015.

[30] Matthias Haase and Tore Wigenstad. Double-skin facade technology for energy-efficient commercial building refurbishment in Norway. In *Roomvent 2011–12th International Conference on Air Distribution in Rooms, Trondheim*, 2011.

[31] Maria Konstantoglou and Aris Tsangrassoulis. Dynamic operation of daylighting and shading systems: A literature review. *Renewable and Sustainable Energy Reviews*, 60:268–283, 2016.

[32] American Society of Heating, Refrigerating and Air-Conditioning Engineers. *2009 ASHRAE Handbook: Fundamentals*. American Society of Heating, Refrigerating and Air-Conditioning Engineers, Atlanta, GA, USA, 2009.

[33] Ignacio Acosta, Miguel Ángel Campano, and Juan Francisco Molina. Window design in architecture: Analysis of energy savings for lighting and visual comfort in residential spaces. *Applied Energy*, 168:493–506, 2016.